IRANIAN JOURNAL OF CATALYSIS

The use of recyclable magnetic nanocatalyst $Fe_3O_4@SiO_2$-$(CH_2)_3$-Pyridine-2-(1H)-tetrazole-Cu(II) in the synthesis of bis-coumarin derivatives under green conditions

Ali Oji Moghanlou*[a]; Mohammadali Pourshahi[a]; Siamak Atabak[a], Nayer Mohammadian Tarighi[a]

a) Department of Chemistry, Ardabil Branch, Islamic Azad University, Ardabil, Iran, 56157-31567

Received 26 March 2023; received in revised form 20 June 2023; accepted 29 June 2023 **(DOI: 10.30495/IJC.2023.1982870.2000)**

ABSTRACT

In the present work, first, magnetic nanoparticles (MNP) were synthesized, and a layer of silica was placed on the magnetite nanoparticles through the reaction with TEOS. Next, the pyridine-2-(1H)-tetrazole ligand was fixed on the core-shell magnetite nanoparticles, and finally, the nanocatalyst copper complex was synthesized. The synthesized copper (II) complex of magnetic nanocatalyst was identified through different analyses such as FT-IR, SEM, EDX, XRD, VSM, BET, and atomic absorption. After characterizing the nanocatalyst $Fe_3O_4@SiO_2$-$(CH_2)_3$-Pyridine-2-(1H)-tetrazole-Cu(II), by applying this catalyst in the reaction of benzaldehyde with 4-hydroxycoumarin, the reaction conditions such as solvent type, reaction temperature and The amount of catalyst was optimized. Ethanol was chosen as the optimal solvent as an environmentally friendly solvent. The recycling cycle of the magnetic catalyst was also studied, and the slight decrease in the catalyst's efficiency after six times reactions indicates the high efficiency of this nanocatalyst in the synthesis reaction of bis-coumarin derivatives as a green catalyst.

***Keywords**: Coumarin; Bis-coumarin; Aldehyde; Magnetic nanocatalyst; Copper catalyst.*

1. Introduction

The focus of green chemistry is on performing chemical reactions with the most negligible impact on the environment. In order to achieve this goal, a lot of effort is needed to advance in the catalytic fields. This indicates the high importance of catalysts to achieve green chemistry goals. Catalyst recycling and their reuse through old methods is a severe problem in the path of achieving the goals of green chemistry. For this purpose, in the past decades, the use of magnetic nanocatalysts has been taken into consideration due to their easy separation [1, 2]. In order to solve this problem and prevent the oxidation of Fe^{2+}, which reduces the magnetic properties of nanoparticles, various mineral and polymer coatings are used. Among different coatings, due to high porosity, high surface area, very low toxicity, and the ability to modify surface silanol groups with various functional groups, silica coatings are widely used [3-6].

*Corresponding author:
E-mail address: *Ali.Oji1972@iau.ac.ir* (**A. O. Moghanlou**)

Based on their unique physical and chemical properties, magnetic nanoparticles are used in various biological fields, such as image enhancement in MRI, tissue repair, immunoassays, biological fluid detoxification, heat therapy, drug delivery, and cell isolation [7-13]. The synthesis methods of magnetic nanoparticles play an important role in determining the morphology (shape, size, and size distribution), composition, magnetic properties, surface properties, and catalytic applications of nanoparticles. Several methods have been invented to make magnetic nanoparticles; among the standard methods are co-precipitation [14-17], microemulsion [18], sol-gel method [19, 20], spray and laser pyrolysis, hydrothermal reaction [21, 22], microwave radiation, and biological synthesis. Among these methods, sol-gel and co-precipitation are more important [23].

Coumarins are a class of heterocyclic compounds that have been noticed due to their various applications in the perfumery, pharmaceutical, and agrochemical

industries [24, 25]. Among the various coumarin derivatives, bis-coumarins are of great importance due to their unique medicinal and biological properties [26, 27]. Bis-coumarin derivatives form an essential part of the structure of heterocyclic drugs that have important biological activities [28]. Bis-coumarins have wide applications as anticoagulant, antibiotic, antimicrobial, antitumor, anti-HIV, and anti-fever drugs. In addition, some bis-coumarin derivatives are used as additives in cosmetics and food products, and these derivatives are used in the manufacture of fluorescent and colorimetric sensors as well as luminescent agents [26, 29-34]. Some of the pharmaceutical structures related to coumarins and bis-coumarins are shown in **Fig. 1**. Dicoumarol (1), warfarin (2), and acenocoumarol (3) are the structures used as natural anticoagulants [35]. Also, the structure of 4, which is called aminocoumarin, is used as an antibiotic for the treatment of staphylococcal infections [36].

In this project, magnetic nanocatalyst Fe_3O_4@SiO_2-$(CH_2)_3$-Pyridine-2-tetrazole-Cu(II) was synthesized as a catalyst with high recovery capability and green. In order to use heterogeneous and magnetic nanocatalysis, we first synthesized magnetite nanoparticles, then using 3-chloropropyltrimethoxysilane as a linker, 2-pyridine tetrazole was fixed on the magnetic substrate, and using $Cu(OAc)_2$, nanocatalyst Fe_3O_4@SiO_2-$(CH_2)_3$-Pyridine-2-tetrazole-Cu(II) was synthesized. In the continuation of the research work, a green method with high efficiency for the synthesis of bis-coumarin derivatives as active medicinal compounds will be provided using this catalyst (**Scheme 1**).

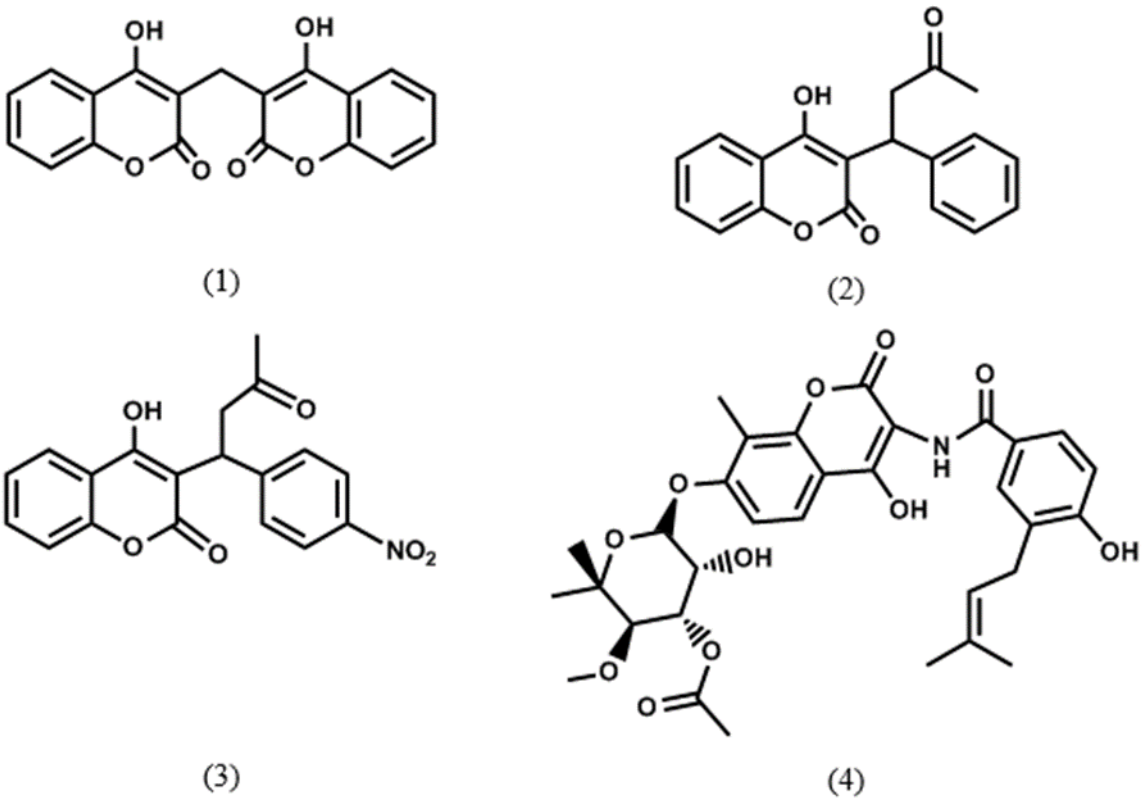

Fig. 1. Coumarin and bis-coumarin pharmaceutical derivatives.

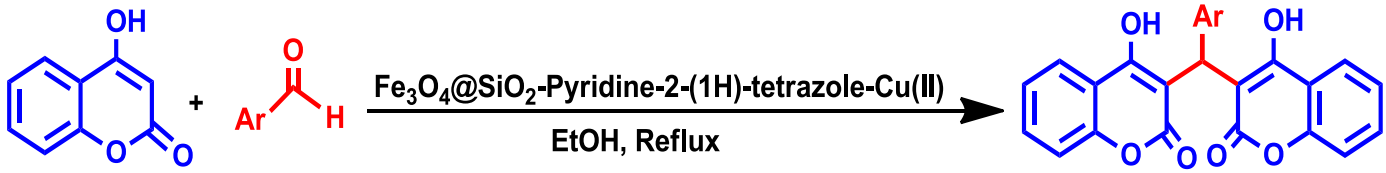

Scheme 1. The synthesis of bis-coumarin derivatives.

2. Experimental

2.1. Materials

(3-chloropropyl)trimethoxysilane and ammonium chloride were purchased from Exir (Austria). The dry solvents were dried according to the methods described in different papers [37]. The other chemicals used in this article were obtained from Merck.

2.2. General protocol for the synthesis of the Fe_3O_4@SiO_2-$(CH_2)_3$- Pyridine-2-(1H)-tetrazole -Cu(II)

2.2.1. Pyridine-2-(1H)-tetrazole synthesis

For the synthesis of Pyridine-2-(1H)-tetrazole into a 100 ml round bottom flask containing 30 ml of dry DMF, pyridine-2-carbonitrile (5.000 g, 48.80 mmol), ammonium chloride (3.350 g, 62.50 mmol) and sodium azide (4.060 g, 62.50 mmol) were added. The mixture was refluxed for 17 h with vigorous stirring. After the completion of the reaction time, the reaction mixture was cooled to room temperature, and the contents of the flask were added to the Erlenmeyer flask containing 150 ml of distilled water, with the gradual addition of concentrated hydrochloric acid, the pH of the mixture reached 2, and the precipitate of the product was formed. The precipitate was filtered under a vacuum and washed with distilled water. Using ethanol (95%), the precipitate was recrystallized to obtain white crystals as a pure product with an efficiency of 54%. The melting temperature of the obtained crystals was measured as 216-218 ℃ [38].

2.2.2. Fe_3O_4@SiO_2@$(CH_2)_3Cl$ synthesis

Silica-coated magnetite nanoparticles were synthesized according to the published article in this field [39, 40]. In the next step, 2.000 g of Fe_3O_4@SiO_2 and 6.67 mmol of (3-chloropropyl)trimethoxysilane was added to the flask containing 50 ml of dry toluene, and stirred for 12 hours under nitrogen and reflux temperature. The formed Fe_3O_4@SiO_2@$(CH_2)_3Cl$ was separated by an external magnet and washed with toluene, and dry ethanol and dried at 80°C for 8 hours [41].

2.2.3. Fe_3O_4@SiO_2-$(CH_2)_3$- Pyridine-2-(1H)-tetrazole -Cu(II) synthesis

Pyridine-2-(1H)-tetrazole (0.588 g, 4.0 mmol) and K_2CO_3 (0.552 g, 4.0 mmol) were added to 30 ml of DMF containing 2 g of Fe_3O_4@SiO_2@$(CH_2)_3Cl$. The reaction mixture was stirred for 24 hours at reflux temperature. The synthesized material was removed from the reaction medium with a magnet and washed repeatedly with DMF, distilled water, and ethanol, and finally dried at 80°C for 8 hours [41]. In the last step, Fe_3O_4@SiO_2-$(CH_2)_3$- Pyridine-2-(1H)-tetrazole was complexed with copper(II) using a solution of $Cu(OAc)_2$ in acetonitrile, and the catalyst Fe_3O_4@SiO_2-$(CH_2)_3$- Pyridine-2-(1H)-tetrazole -Cu(II) was synthesized.

2.3. Synthesis of bis-coumarin derivatives

1.0 mmol of aldehyde and 2.0 mmol of 4-hydroxycoumarin were added to a flask (10 ml) containing ethanol as a reaction solvent, and then 50 mg of the catalyst Fe_3O_4@SiO_2-$(CH_2)_3$- Pyridine-2-(1H)-tetrazole-Cu(II) was added to the reaction vessel. The reaction was stirred at reflux temperature. The progress of the reaction was checked by TLC in an n-hexane/EtOAc/MeOH solvent mixture with a ratio of 5:2:1. After making sure that the reactants were consumed, the heterogeneous catalyst was removed from the reaction vessel with a magnet. The reaction product was extracted with dichloromethane. Other bis-coumarin derivatives were synthesized via the procedure described above.

2.4. Catalyst recovery

The nanocatalyst was removed from the contents of the reaction vessel using a magnet, repeatedly washed with ethanol and acetone, dried, and catalyzed the subsequent reactions again.

3. Results and Discussion

3.1. Preparation and characterization of the catalyst

Magnetite nanoparticles coated with silica were synthesized according to the method reported in different articles and identified through common analyses. Next, in dry toluene, 3-chloropropyltrimethoxysilane was stabilized on Fe_3O_4@silica core shells. The synthesized pyridine-2-(1H)-tetrazole reacted with Fe_3O_4@SiO_2@$(CH_2)_3Cl$ in the presence of K_2CO_3 and DMF as reaction solvent, and the compound Fe_3O_4@SiO_2@$(CH_2)_3$-Pyridine-2-(1H)- tetrazole was synthesized. In the last step, the copper (II) complex of the magnetic nanocatalyst was obtained using a solution of $Cu(OAc)_2$ in acetonitrile (**Scheme 2**). The copper content (0.36 mmol g^{-1}) was measured by atomic absorption analysis.

FT-IR analysis was used to investigate the processes performed during different stages of catalyst synthesis and to confirm the structure and formation of Fe_3O_4@SiO_2-$(CH_2)_3$ Pyridine-2-(1H)-tetrazole-Cu (II) magnetic nanocatalyst (**Fig. 2**).

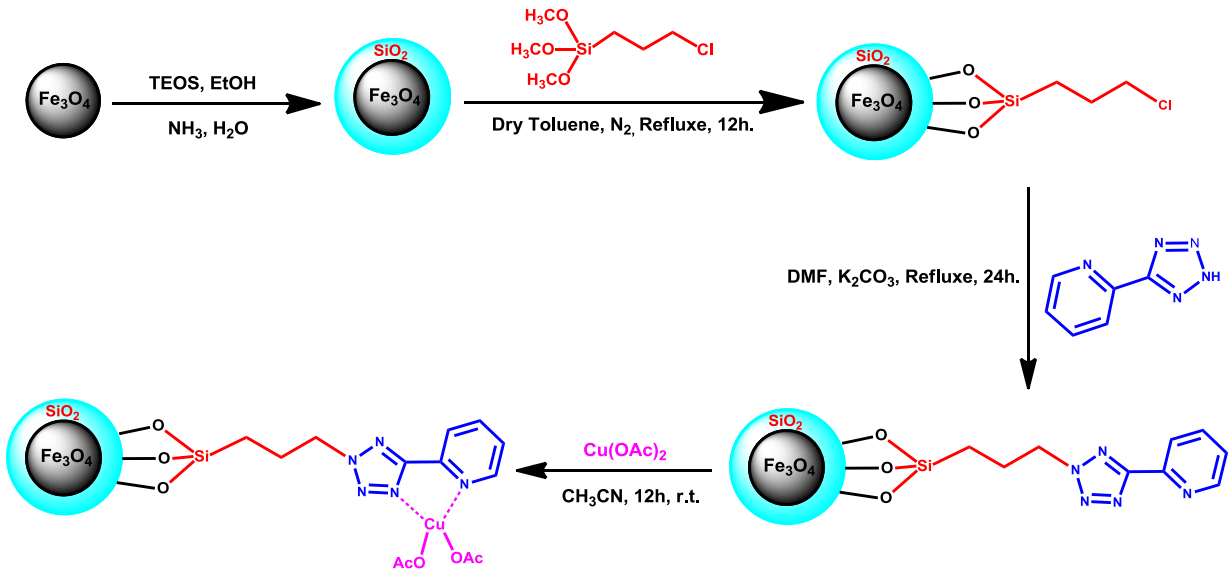

Scheme 2. Synthesis of Fe_3O_4@SiO_2-$(CH_2)_3$-Pyridine-2-(1H)-tetrazole -Cu(II).

In **Fig. 2a-c**, the broad peak in the 3600-3100 cm^{-1} corresponds to the O-H stretching vibration. A double peak at 578 cm^{-1} and 650 cm^{-1} (**Fig. 2a**) indicates the formation of Fe_3O_4, and the absorption peak at 578 cm^{-1} indicates the Fe-O vibration. The peaks in 808 cm^{-1} and 952 cm^{-1} are attributed to Si-O bending and Si-OH stretching vibrations. A strong absorption band at 1090 cm^{-1} is proof of the stretching vibration of the Si-O-Si bond, which indicates the correct coating of magnetite nanoparticles with a silica shell. Also, the absorption peaks at 1656 cm and 1422 cm can be attributed to the stretching vibrations of C=C and C=N bonds and the scissor vibration of CH_2 (**Fig. 2b**). It should be noted that the peaks related to stretching vibrations of C=C and C=N bonds and CH_2 scissor vibration in **Fig. 2b** have shifted to low frequencies, which can be considered a reason for the complexation of the ligand with copper [41]. SEM images of magnetite nanoparticles and magnetic catalyst Fe_3O_4@SiO_2-$(CH_2)_3$ Pyridine-2-(1H)-tetrazole-Cu(II) are shown in **Fig. 3.** By studying these images, it can be seen that the size of the particles is smaller than 100 nm.

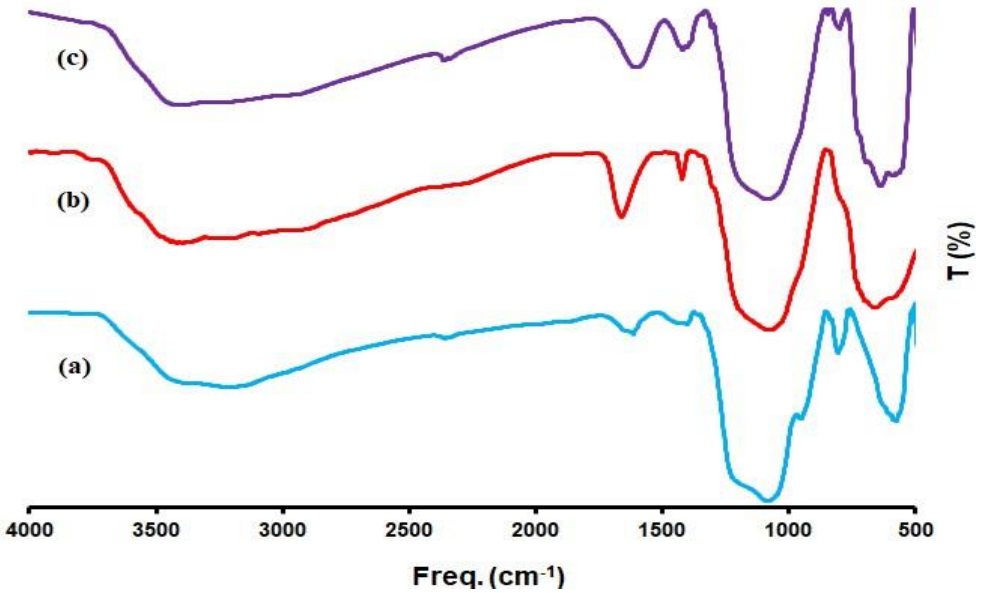

Fig. 2. FT-IR spectra (Neet) of: (a) Fe_3O_4@SiO_2; (b) Fe_3O_4@SiO_2-$(CH_2)_3$-Pyridine-2-(1H)-tetrazole; (c) Fe_3O_4@SiO_2-$(CH_2)_3$-Pyridine-2-(1H)-tetrazole -Cu(II).

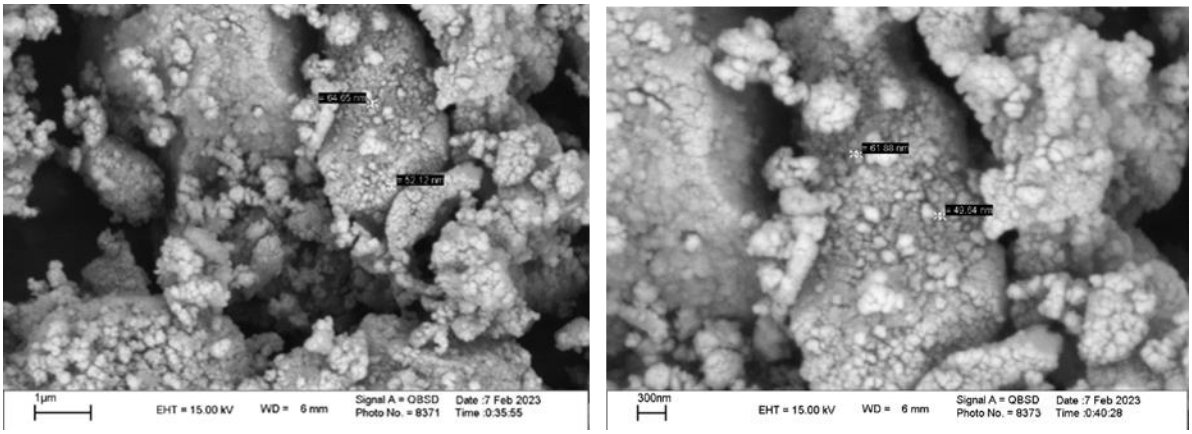

Fig. 3. SEM images of magnetic nanocatalyst Fe_3O_4@SiO_2-$(CH_2)_3$-Pyridine-2-(1H)-tetrazole-Cu(II).

In **Fig. 4**, the graph related to TGA analysis of coated magnetite nanoparticles and synthesized nanocatalysts is shown. The weight loss up to 220 °C in magnetite and nanocatalyst is due to the removal of water and other solvents used during the synthesis of the nanocatalyst. From the temperature of 230-535 °C, a weight loss is observed, which is due to the thermal decomposition of the organic ligand stabilized on the magnetite nanoparticles.

The XRD pattern of magnetite nanoparticles and Fe_3O_4@SiO_2-$(CH_2)_3$-Pyridine-2-(1H)-tetrazole-Cu(II) in the region of 2θ=10-80° is shown in **Fig. 5.** By studying the XRD pattern of magnetite nanoparticles and magnetic nanocatalyst (5a and 5b), it was observed that the peaks in the regions of 2θ= 30.35°, 35.95°, 43.45°, 53.70°, 57.25° and 62.88° which were characterized by Miller indices (220), (311), (400), (422), (511) and (440), indicates the crystal structure of inverted spinel with space group Fd-3m for magnetite nanoparticles and magnetic nanocatalyst. Which corresponds to the JCPDS reference No. 0417-79. The absence of additional peaks indicates the high purity of the synthesized compound.

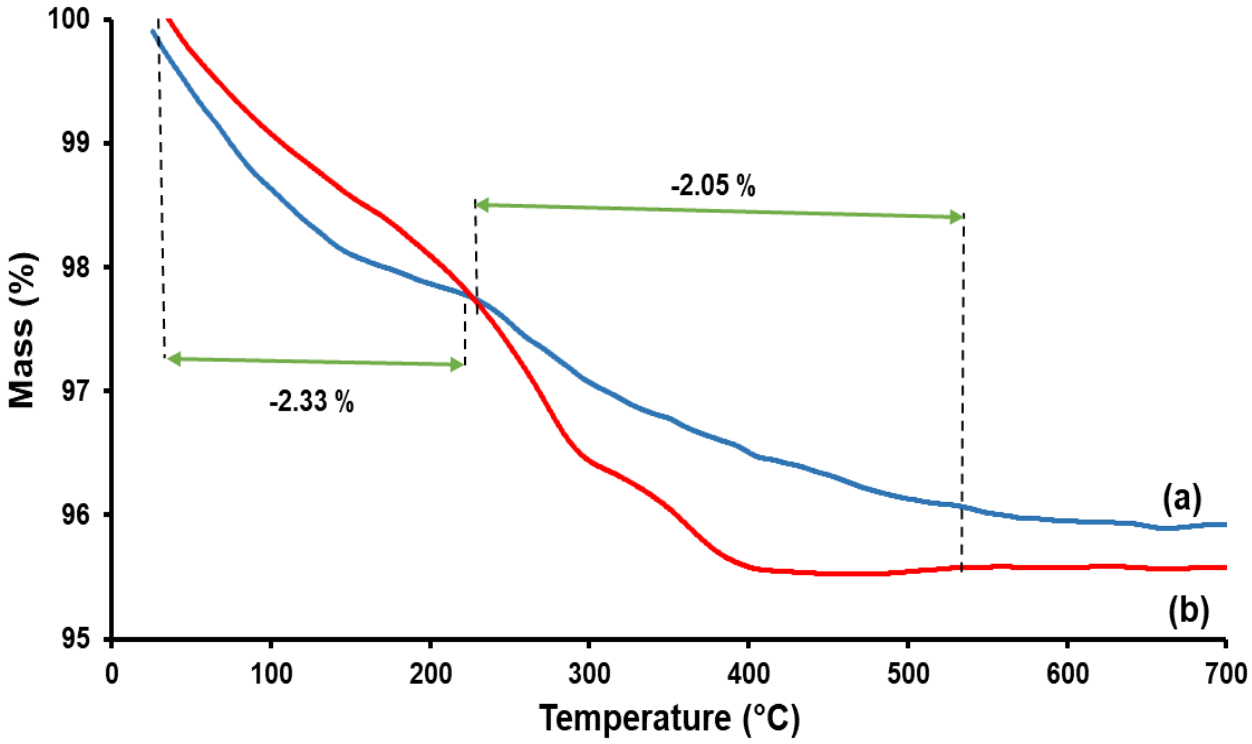

Fig. 4. TGA curve of a) Fe_3O_4@SiO_2 nanoparticles; b) Fe_3O_4@SiO_2-$(CH_2)_3$-Pyridine-2-(1H)-tetrazole-Cu(II) (under N_2 atmosphere, scan rate 10ºC /min).

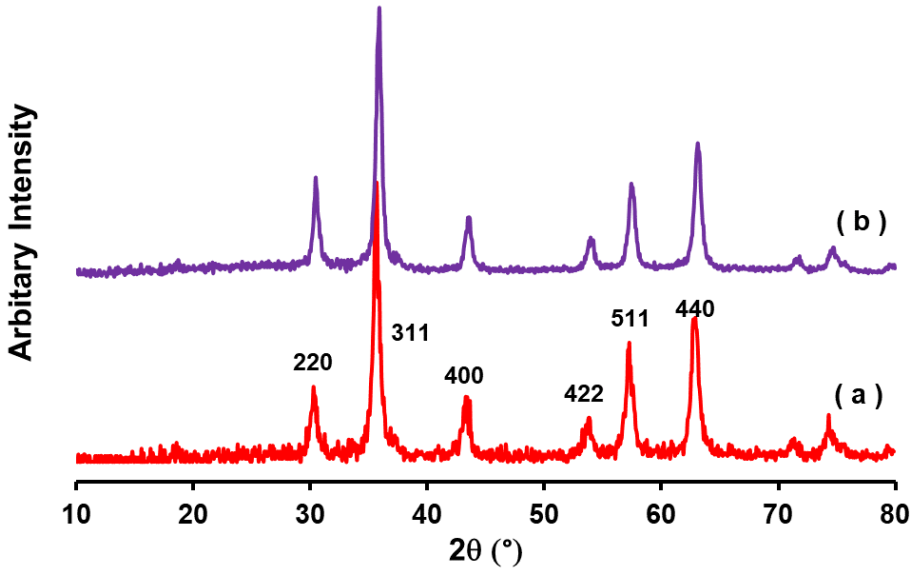

Fig. 5. XRD pattern: a) magnetite; b) Fe_3O_4@SiO_2-$(CH_2)_3$-Pyridine-2-(1H)-tetrazole-Cu(II).

Vibrating sample magnetometer (VSM) analysis was used to investigate the magnetic properties of coated magnetite nanoparticles and Fe_3O_4@SiO_2-$(CH_2)_3$-Pyridine-2-(1H)-tetrazole-Cu(II) nanocatalyst. VSM analysis was performed at 298 K and with magnetic field scanning from -12500 to +12500 Oe for magnetic samples, and the related curve is shown in Figure 6. The interpretation and study of **Fig. 6** show the superparamagnetic property of Fe_3O_4@SiO_2 nanoparticles and Fe_3O_4@SiO_2-$(CH_2)_3$-Pyridine-2-(1H)-tetrazole-Cu(II) nanocatalyst. Also, due to the high superparamagnetic property of the nanocatalyst, the synthesized magnetic catalyst can be easily separated from the reaction medium with a magnet.

Energy dispersive X-ray spectroscopy (EDS) analysis was used to study the composition of nanocatalyst elements. The EDS spectrum (**Fig. 7**) confirms the presence of Fe, Si, N, C, O and Cu elements in the synthesized catalyst composition.

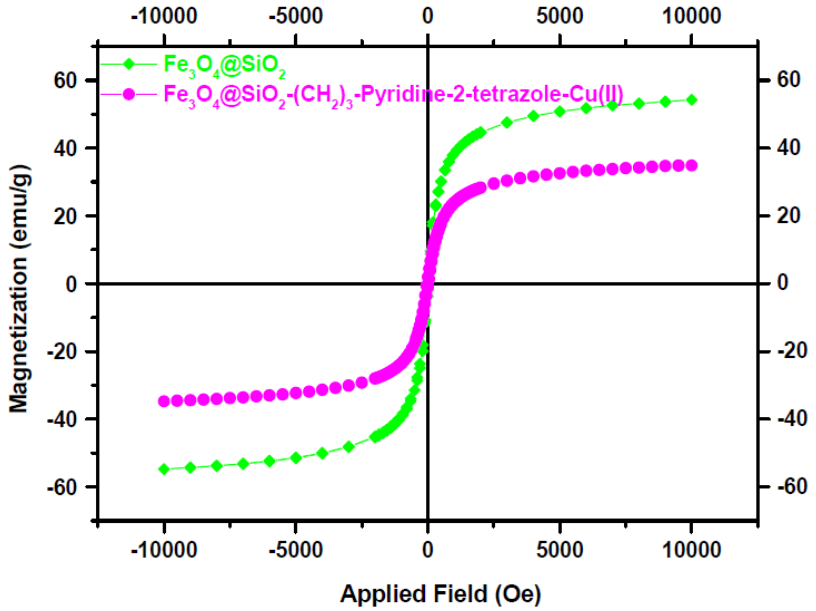

Fig. 6. Magnetometry curve, Fe_3O_4@SiO_2 nanoparticles and Fe_3O_4@SiO_2-$(CH_2)_3$-Pyridine-2-(1H)-tetrazole-Cu(II).

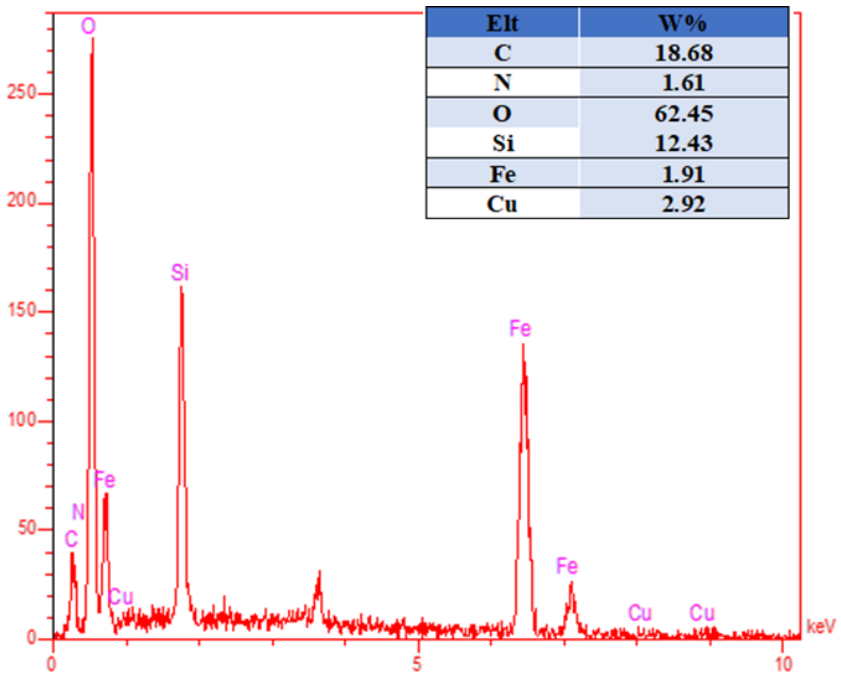

Fig. 7. The EDS spectra of Fe_3O_4@SiO_2-$(CH_2)_3$-Pyridine-2-(1H)-tetrazole-Cu(II).

3.2. Synthesis of bis-coumarin derivatives

To optimize the synthesis conditions of bis-coumarin derivatives, the reaction between benzaldehyde (1.0 mmol) and 4-hydroxycoumarin (2.0 mmol) was selected as a model reaction. Different reaction conditions such as type of solvent, amount of catalyst, and temperature were investigated (the results obtained are summarized in **Table 1**). Solvent screening of the reaction (entries 1-7) indicates that the reaction has a high efficiency in polar protic solvents such as water (entry 1, 70% conversion) and ethanol (entry 7, 94% conversion). As an environmentally friendly solvent, ethanol was selected as the optimum solvent. Also, the reaction in solvent-free conditions (entry 14) had poor conversion. As can be seen in **Table 1**, the amount of 50 mg of catalyst shows the highest efficiency for this reaction (entry 7, 94% conversion), and in amounts less than 50 mg (entries 8-9), moderate conversions are observed. At high amounts of catalyst (entry 10), a very small increase in reaction efficiency is observed. It should be noted that the reaction had low efficiency in the absence of a catalyst (entry 11). Also, the reaction temperature was optimized (entry 7, 12-13), and the reflux temperature (entry 7) was chosen as the optimal temperature. In addition, the reaction was performed in the presence of $Cu(OAc)_2$ (entry 15), Fe_3O_4@SiO_2 (entry 16) and Fe_3O_4@SiO_2-$(CH_2)_3$-Pyridine-2-(1H)-tetrazole (entry 17) as catalysts. The obtained efficiencies show the high efficiency of $Cu(OAc)_2$ (95%) compared to Fe_3O_4@SiO_2 and Fe_3O_4@SiO_2-$(CH_2)_3$-Pyridine-2-(1H)-tetrazole for carrying out the reaction of bis-coumarin derivatives synthesis.

A wide range of aldehyde derivatives was used for the synthesis of bis-coumarin derivatives, and the results are summarized in **Table 2**. The purified products were identified by melting point measurements and FT-IR and NMR spectra. By comparing the reaction efficiency of different aldehyde derivatives and the synthesis time of bis-coumarin derivatives, it can be said that the presence of electron-withdrawing and electron-donating substitutions in aldehyde has a very small effect on the reaction rate.

Based on various articles in **Scheme 3**, a mechanism for the synthesis of bis-coumarin derivatives with the catalyst Fe_3O_4@SiO_2-$(CH_2)_3$-Pyridine-2-(1H)-tetrazole-Cu(II) is proposed. As can be seen, in this mechanism, copper acts as a Lewis acid and activates the carbonyl group in aldehydes and intermediates. In the first step, as a result of the nucleophilic attack of 4-hydroxycoumarin on the aldehyde activated by the catalyst, intermediate (A) is formed, which is then converted to compound (B) by losing H_2O. Compound (B) is reactivated by the catalyst and reacts again with 4-hydroxycoumarin through the Michael addition reaction, and compound (c) is obtained. In the last step, compound (C) becomes the final product during the tautomerization process [26, 36, 51].

Table 1. Optimization for bis-coumarin synthesis from benzaldehyde with 4-hydroxycoumarin.[a]

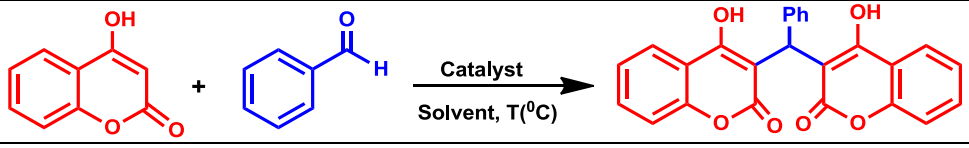

Entry	Solvent	T (°C)	Cat. (mg)	Conversion (%)
1	H_2O	Reflux	50.0	70
2	THF	Reflux	50.0	55
3	Toluene	Reflux	50.0	63
4	CH_3Cl	Reflux	50.0	25
5	CH_3CN	Reflux	50	45
6	EtOH/H_2O (1:1)	Reflux	50.0	82
7	EtOH	Reflux	50.0	94
8	EtOH	Reflux	30.0	60
9	EtOH	Reflux	40.0	77
10	EtOH	Reflux	60.0	95
11	EtOH	Reflux	-	20
12	EtOH	50	50.0	45
13	EtOH	70	50.0	82
14	-	80	50.0	30
15	EtOH	Reflux	50.0 ($Cu(OAc)_2$)	95
16	EtOH	Reflux	50.0 ($Fe_3O_4@SiO_2$)	78
17	EtOH	Reflux	50.0 ($Fe_3O_4@SiO_2$-$(CH_2)_3$-Pyridine-2-(1H)-tetrazole)	54

a)Optimal reaction conditions are in bold.
b) Reaction conditions: Aldehyde (1.0 mmol); 4- hydroxycoumarin (2.0 mmol); solvent (3.0 mL); and reaction time 80 min.

Table 2. Synthesis of bis-coumarin derivatives from aromatic aldehydes with 4-hydroxycoumarin using nanocatalyst $Fe_3O_4@SiO_2$-$(CH_2)_3$-Pyridine-2-(1H)-tetrazole-Cu(II).[a]

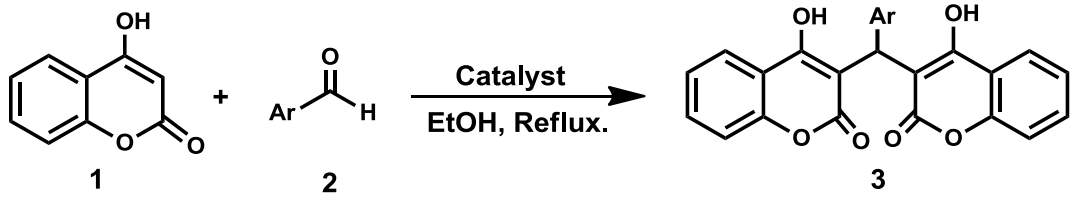

Entry	Substrate	Product	Time (min)	m.p. (°C) Found	m.p. (°C) Reported [Ref.]	Yield (%)[b]
1	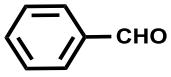	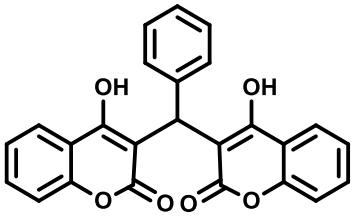	80	230-233	230-232 [42]	94
2	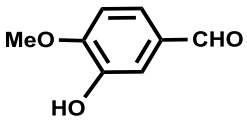	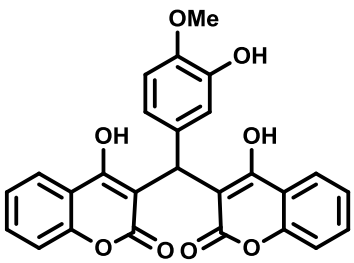	100	240-244	240-242 [43]	87

3	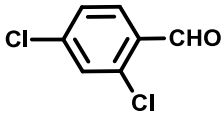	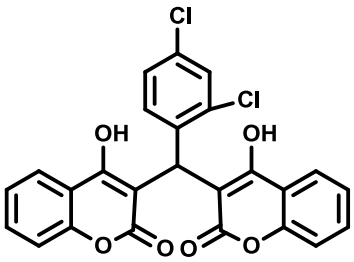	80	192-194	190-195 [44]	90
4	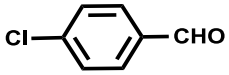	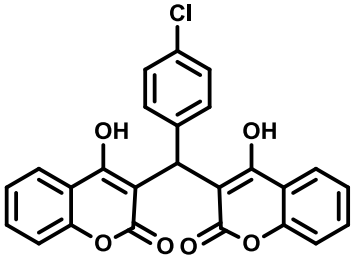	80	201-203	201-201 [45]	90
5	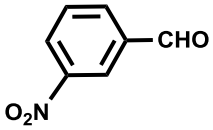	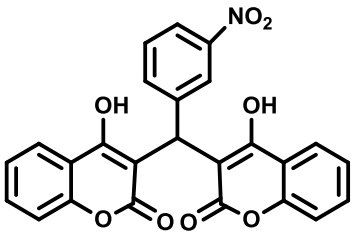	70	213-215	214-216 [46]	93
6	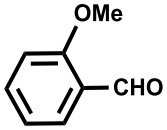	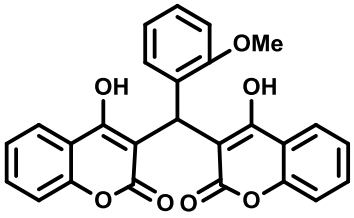	120	211-213	213-215 [44]	95
7	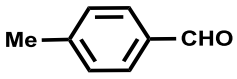	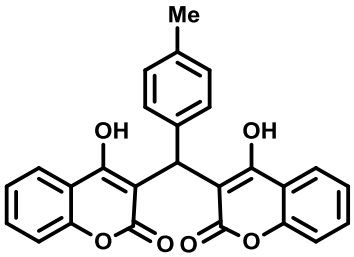	50	265-268	265-267 [47]	89
8	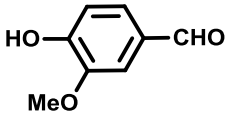	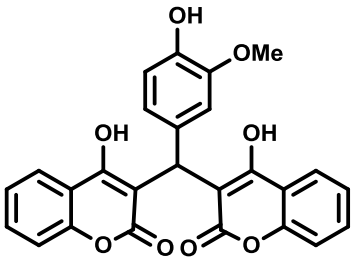	120	225-228	226-227 [33]	87
9		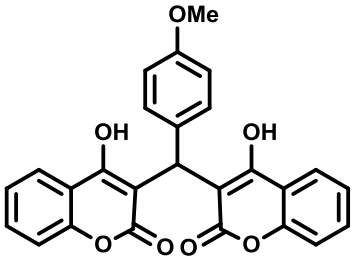	100	251-254	250-252 [48]	90

10	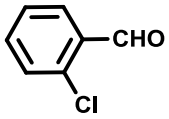	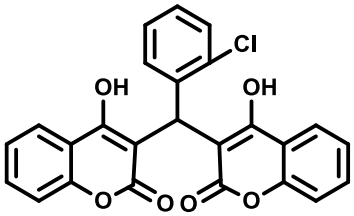	90	201-204	202-205 [49]	91
11	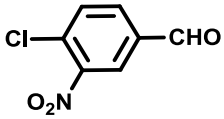	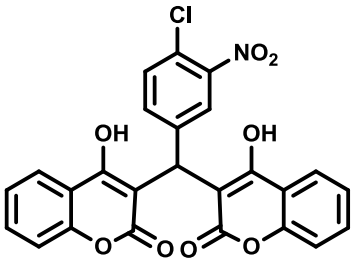	110	250-253	250-252 [50]	91

a) Reaction conditions: Aldehyde (1.0 mmol); 4- hydroxycoumarin (2.0 mmol); solvent (3.0 mL) and catalyst (50 mg).
b) Yields are given for isolated products.

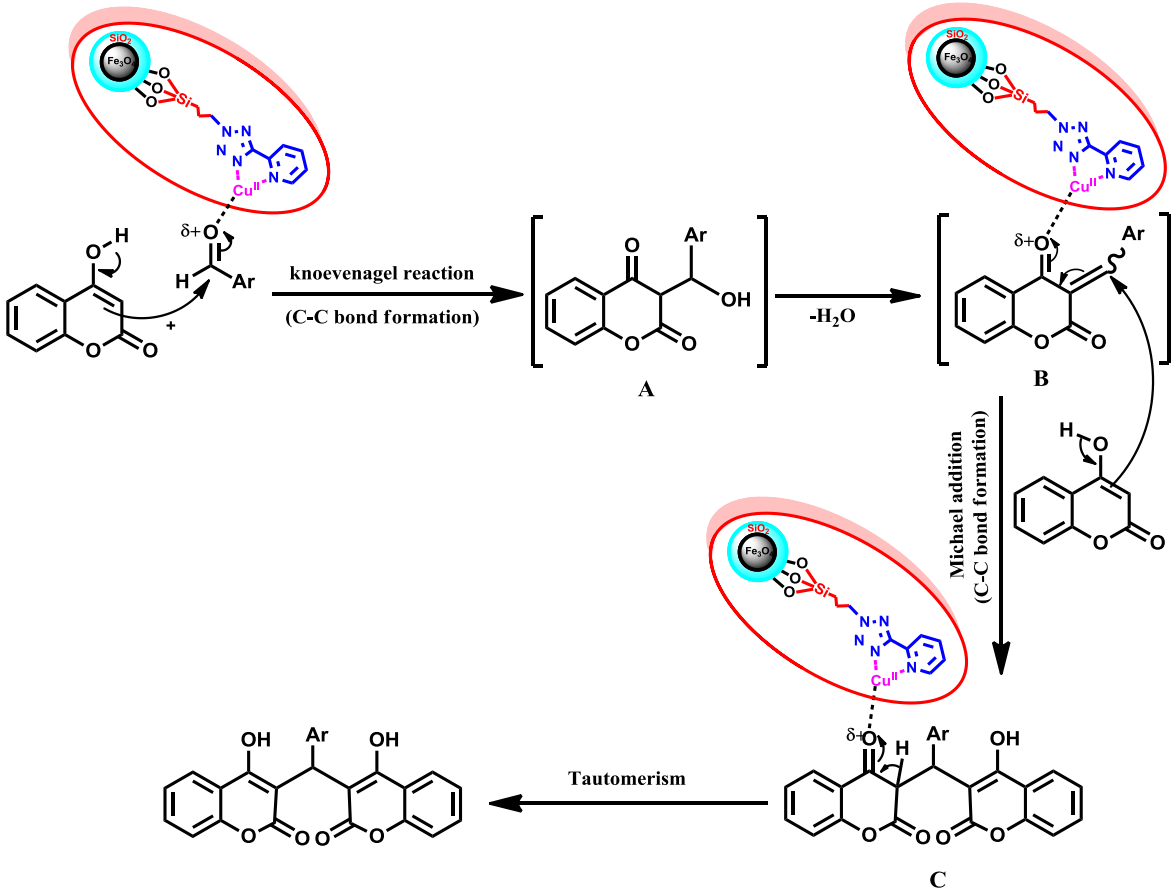

Scheme 3. Proposed mechanism for the synthesis of bis-coumarin derivatives in the presence of Fe_3O_4@SiO_2-$(CH_2)_3$-Pyridine-2-(1H)-tetrazole-Cu(II).

3.3. Recyclability

By applying the catalyst in several consecutive reactions of benzaldehyde with 4-hydroxycoumarin, the reusability of nanocatalyst Fe_3O_4@SiO_2-$(CH_2)_3$-Pyridine-2-(1H)-tetrazole-Cu(II) in the synthesis of bis-coumarin derivatives was investigated, **Fig. 8**. After each reaction, the magnetic nanocatalyst was separated from the reaction mixture by a magnet, washed with ethanol several times, and after drying, it was used in the subsequent reaction. By looking at **Fig. 8**, it can be seen that this nanocatalyst has lost only 4% of its initial activity after six times of reaction.

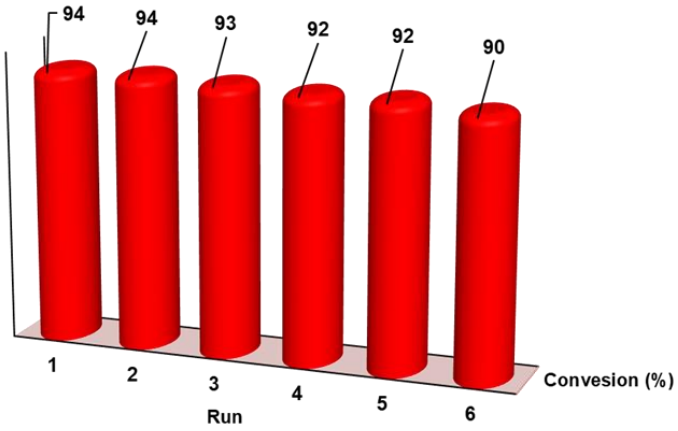

Fig. 8. Recycling diagram of magnetic catalyst Fe_3O_4@SiO_2-$(CH_2)_3$-Pyridine-2-(1H)-tetrazole-Cu(II) in the reaction of bis-coumarin derivatives synthesis.

Therefore, Fe_3O_4@SiO_2-$(CH_2)_3$-Pyridine-2-(1H)-tetrazole-Cu(II) can be mentioned as an effective catalyst with high recyclability in the synthesis of various bis-coumarin derivatives.

4. Conclusions

Briefly, pyridine-4-tetrazole was immobilized on core-shell magnetite nanoparticles. Next, using $Cu(OAc)_2$ solution in acetonitrile, nanocatalyst Fe_3O_4@SiO_2-$(CH_2)_3$-Pyridine-2-(1H)-tetrazole-Cu(II) was synthesized. The synthesized heterogeneous catalyst was used in the reaction of the synthesis of bis-coumarin derivatives through the reaction between 4-hydroxycoumarin and different aromatic aldehydes. The use of Fe_3O_4@SiO_2-$(CH_2)_3$-Pyridine-2-(1H)-tetrazole-Cu(II) catalyst increased the reaction efficiency and carried out the reaction in mild conditions and ethanol as a green solvent. Easy removal from the reaction mixture without time-consuming and expensive methods and a slight decrease in the catalyst's efficiency in the reuse of the catalyst have been used from the advantages of the heterogeneous catalyst.

Acknowledgements

The financial and spiritual support of the Research Council of Islamic Azad University, Ardabil branch is gratefully acknowledged.

References

[1] Y. Wang, X. Wang, M. Antonietti, Polymeric graphitic carbon nitride as a heterogeneous organocatalyst: from photochemistry to multipurpose catalysis to sustainable chemistry, Angew. Chem. Inter. Edit., 51 (2012) 68-89.

[2] M. Ghobadi, M. Kargar Razi, R. Javahershenas, M. Kazemi, Nanomagnetic reusable catalysts in organic synthesis, Synth. Commun., 51 (2021) 647-669.

[3] W. Wu, Q. He, C. Jiang, Magnetic Iron Oxide Nanoparticles: Synthesis and Surface Functionalization Strategies, Nanoscale Res. Lett., 3 (2008) 397.

[4] A.K. Gupta, M. Gupta, Synthesis and surface engineering of iron oxide nanoparticles for biomedical applications, Biomaterials, 26 (2005) 3995-4021.

[5] C. Klein, Hurlburt jr. CS "Manual of Mineralogy", in, New York, John Wiley and Sons, Inc, 1993.

[6] S. Shylesh, V. Schünemann, W.R. Thiel, Magnetically Separable Nanocatalysts: Bridges between Homogeneous and Heterogeneous Catalysis, Angew. Chem. Inter. Edit., 49 (2010) 3428-3459.

[7] A.S. Arbab, L.A. Bashaw, B.R. Miller, E.K. Jordan, B.K. Lewis, H. Kalish, J.A. Frank, Characterization of biophysical and metabolic properties of cells labeled with superparamagnetic iron oxide nanoparticles and transfection agent for cellular MR imaging, Radiology, 229 (2003) 838-846.

[8] P. Reimer, R. Weissleder, [Development and experimental use of receptor-specific MR contrast media], Der Radiologe, 36 (1996) 153-163.

[9] M. Esmaeilpour, A.R. Sardarian, J. Javidi, Synthesis and characterization of Schiff base complex of Pd (II) supported on superparamagnetic Fe3O4@ SiO2 nanoparticles and its application as an efficient copper- and phosphine ligand-free recyclable catalyst for Sonogashira–Hagihara coupling reactions, J. Organometal. Chem., 749 (2014) 233-240.

[10] M. Esmaeilpour, J. Javidi, F.N. Dodeji, M.M. Abarghoui, Facile synthesis of 1-and 5-substituted 1H-tetrazoles catalyzed by recyclable ligand complex of copper (II) supported on superparamagnetic Fe3O4@ SiO2 nanoparticles, J. Mol. Catal. A: Chem., 393 (2014) 18-29.

[11] M. Sarkheil, M. Lashanizadegan, M. Ghiasi, High catalytic activity of magnetic Fe3O4@ SiO2-Schiff base-Co (II) nanocatalyst for aerobic oxidation of alkenes and alcohols and DFT study, J. Mol. Struct., 1179 (2019) 278-288.

[12] M. Rezaei, K. Azizi, K. Amani, Copper–birhodanine complex immobilized on Fe3O4 nanoparticles: DFT studies and heterogeneous catalytic applications in the synthesis of propargylamines in aqueous medium, Appl. Organometal. Chem., 32 (2018) e4120.

[13] L. Vahabi, P.R. Ranjbar, F. Davar, Cladosporium protease/doxorubicin decorated Fe3O4@ SiO2 nanocomposite: An efficient nanoparticle for drug delivery and combating breast cancer, J. Drug Deliv. Sci. Tech., 80 (2023) 104144.

[14] A.-H. Lu, E.L. Salabas, F. Schüth, Magnetic Nanoparticles: Synthesis, Protection, Functionalization, and Application, Angew. Chem. Inter. Edit., 46 (2007) 1222-1244.

[15] G. Huang, C.-H. Lu, H.-H. Yang, Chapter 3 - Magnetic Nanomaterials for Magnetic Bioanalysis, in: X. Wang, X. Chen (Eds.) Novel Nanomaterials for Biomedical, Environmental and Energy Applications, Elsevier, 2019, pp. 89-109.

[16] G. Gnanaprakash, S. Mahadevan, T. Jayakumar, P. Kalyanasundaram, J. Philip, B. Raj, Effect of initial pH and temperature of iron salt solutions on formation of magnetite nanoparticles, Mater. Chem. Physic., 103 (2007) 168-175.
[17] A. Khalid, R. Ahmed, M. Taha, T. Soliman, Fe3O4 nanoparticles and Fe3O4@ SiO2 core-shell: synthesize, structural, morphological, linear, and nonlinear optical properties, J. Alloy. Comp., 947 (2023) 169639.
[18] B.K. Paul, S.P. Moulik, Uses and applications of microemulsions, Current Science, 80 (2001) 990-1001.
[19] C. Graf, D.L. Vossen, A. Imhof, A. van Blaaderen, A general method to coat colloidal particles with silica, Langmuir, 19 (2003) 6693-6700.
[20] M. Mohapatra, S. Anand, Synthesis and applications of nano-structured iron oxides/hydroxides–a review, International J. Eng., Sci. Tech., 2 (2010).
[21] S. Giri, S. Samanta, S. Maji, S. Ganguli, A. Bhaumik, Magnetic properties of α-Fe2O3 nanoparticle synthesized by a new hydrothermal method, J. Magnet. Magnet. Mater, 285 (2005) 296-302.
[22] Z. Jing, S. Wu, Synthesis and characterization of monodisperse hematite nanoparticles modified by surfactants via hydrothermal approach, Mater. Lett., 58 (2004) 3637-3640.
[23] D. Wang, D. Astruc, Fast-Growing Field of Magnetically Recyclable Nanocatalysts, Chem. Rev., 114 (2014) 6949-6985.
[24] Z. Du, W. Zhou, L. Bai, F. Wang, J.-X. Wang, In Situ Generation of Palladium Nanoparticles: Reusable, Ligand-Free Heck Reaction in PEG-400 Assisted by Focused Microwave Irradiation, Synlett, 2011 (2011) 369-372.
[25] B.B. Shaik, N.K. Katari, P. Seboletswe, R. Gundla, N.D. Kushwaha, V. Kumar, P. Singh, R. Karpoormath, M.D. Bala, Recent Literature Review on Coumarin Hybrids as Potential Anticancer Agents, Anti-Cancer Agents in Medicinal Chemistry (Formerly Current Medicinal Chemistry-Anti-Cancer Agents), 23 (2023) 142-163.
[26] P. Teli, A. Sethiya, S. Agarwal, An insight view on synthetic protocol, mechanistic and biological aspects of biscoumarin derivatives, ChemistrySelect, 4 (2019) 13772-13787.
[27] S. Zeinali, L.Z. Fekri, M. Nikpassand, R.S. Varma, Greener Syntheses of Coumarin Derivatives Using Magnetic Nanocatalysts: Recent Advances, Topics in Current Chemistry, 381 (2023) 1.
[28] F. Borges, F. Roleira, N. Milhazes, L. Santana, E. Uriarte, Simple coumarins and analogues in medicinal chemistry: occurrence, synthesis and biological activity, Current medicinal chemistry, 12 (2005) 887-916.
[29] N.O. Mahmoodi, F. Ghanbari Pirbasti, Z. Jalalifard, Recent advances in the synthesis of biscoumarin derivatives, J. Chin. Chem. Soc., 65 (2018) 383-394.
[30] K. Parvanak Boroujeni, P. Ghasemi, Z. Rafienia, Synthesis of biscoumarin derivatives using poly (4-vinylpyridine)-supported dual acidic ionic liquid as a heterogeneous catalyst, Monatshefte für Chemie-Chemical Monthly, 145 (2014) 1023-1026.
[31] D.S. Reddy, M. Kongot, V. Singh, M.A. Siddiquee, R. Patel, N.K. Singhal, F. Avecilla, A. Kumar, Biscoumarin–pyrimidine conjugates as potent anticancer agents and binding mechanism of hit candidate with human serum albumin, Archiv der Pharmazie, 354 (2021) 2000181.
[32] N.O. Mahmoodi, Z. Jalalifard, G.P. Fathanbari, Green synthesis of bis-coumarin derivatives using Fe (SD) 3 as a catalyst and investigation of their biological activities, J. Chin. Chem. Soc., 67 (2020) 172-182.
[33] M. Faisal, F.A. Larik, A. Saeed, A highly promising approach for the one-pot synthesis of biscoumarins using HY zeolite as recyclable and green catalyst, J. Porous Mater., 26 (2019) 455-466.
[34] P. Li, R. Su, D. Zhang, M. Han, Y. Zhao, L. Ma, H. Zhang, T. Yu, Carbazole-functionalized V-shaped bis-coumarin derivatives as organic luminescent materials, Synthetic Metals, 287 (2022) 117069.
[35] T. Schalekamp, B.P. Brassé, J.F. Roijers, Y. Chahid, J.H. van Geest-Daalderop, H. de Vries-Goldschmeding, E.M. van Wijk, A.C. Egberts, A. de Boer, VKORC1 and CYP2C9 genotypes and acenocoumarol anticoagulation status: interaction between both genotypes affects overanticoagulation, Clinical Pharmacology & Therapeutics, 80 (2006) 13-22.
[36] E. Zarenezhad, M.N. Montazer, M. Tabatabaee, C. Irajie, A. Iraji, New solid phase methodology for the synthesis of biscoumarin derivatives: experimental and in silico approaches, BMC Chemistry, 16 (2022) 53.
[37] W.L.F. Armarego, C.L.L. Chai, Purification of laboratory chemicals, 5th ed., Butterworth-Heinemann, Burlington, 2003.
[38] Y. Mansoori, B. Koohi-Zargar, H. Shekaari, M.R. Zamanloo, G.H. Imanzadeh, Polyamides with pendant 1,3,4-oxadiazole and pyridine moieties, Chin. J. Polymer Sci., 30 (2012) 112-121.
[39] L. Ciccotti, L.A.S. do Vale, T.L.R. Hewer, R.S. Freire, Fe3O4@TiO2 preparation and catalytic activity in heterogeneous photocatalytic and ozonation processes, Catal. Sci. Tech., 5 (2015) 1143-1152.
[40] S. Wang, K. Wang, C. Dai, H. Shi, J. Li, Adsorption of Pb2+ on amino-functionalized core–shell magnetic mesoporous SBA-15 silica composite, Chem. Eng. J., 262 (2015) 897-903.
[41] M. Nasrollahzadeh, Z. Issaabadi, S.M. Sajadi, Fe 3 O 4@ SiO 2 nanoparticle supported ionic liquid for green synthesis of antibacterially active 1-carbamoyl-1-phenylureas in water, RSC adv., 8 (2018) 27631-27644.
[42] H. Mehrabi, H. Abusaidi, Synthesis of biscoumarin and 3, 4-dihydropyrano [c] chromene derivatives catalysed by sodium dodecyl sulfate (SDS) in neat water, J. Iran. Chem. Soc., 7 (2010) 890-894.
[43] P. Teli, A. Sethiya, S. Agarwal, Black yet green: A heterogenous carbon-based acid catalyst for the synthesis of biscyclic derivatives under eco-friendly conditions, Res. Chem. Intermed., 48 (2022) 731-750.

[44] A. Shamsaddini, E. Sheikhhosseini, Synthesis of 3, 3-arylidene bis (4-hydroxycoumarin) catalyzed by p-dodecylbenzenesulfonic acid (DBSA) in aqueous media and microwave irradiation, Inter. J. Org. Chem., 4 (2014) 135-141.
[45] A.D. Gupta, S. Samanta, R. Mondal, A.K. Mallik, A Convenient, Eco-friendly, and Efficient Method for Synthesis of 3, 3'-Arylmethylene-bis-4-hydroxycoumarins, Bullet. Korean Chem. Soc., 33 (2012) 4239-4242.
[46] N. Iravani, M. Keshavarz, M. Mousavi, M. Baghernejad, Melamine trisulfonic acid: An efficient and recyclable solid acid catalyst for the green synthesis of Biscoumarin derivatives, Iran. J. Catal., 5 (2015) 65-71.
[47] S. Zahiri, M. Mokhtary, Bi (NO3) 3· 5H2O: An efficient catalyst for one-pot synthesis of 3-((aryl)(diethylamino) methyl)-4-hydroxy-2H-chromen-2-ones and biscoumarin derivatives, J. Taibah Uni. Sci., 9 (2015) 89-94.
[48] Z. Zare-Akbari, L. Edjali, M. Eshaghi, Synthesis of Novel Bis-Coumarin Derivatives as Potential Acetylcholinesterase Inhibitors: An In Vitro, Molecular Docking, and Molecular Dynamics Simulations Study, Pharmaceutical and Biomedical Research, 8 (2022) 131-142.
[49] Z.M. Mohammadi, N. Mahmoodi, Nano TiO2@ KSF as a high-efficient catalyst for solvent-free synthesis of Biscoumarin derivatives, Int. J. Nano Dimens 7(2) (2016) 174-180.
[50] B. Kharrngi, E.D. Dhar, G. Basumatary, D. Das, R.C. Deka, A.K. Yadav, G. Bez, Developing a highly potent anthelmintic: study of catalytic application of l-proline derived aminothiourea in rapid synthesis of biscoumarins and their in vitro anthelmintic essay, J. Chem. Sci., 133 (2021) 16.
[51] J. Albadi, A. Mansournezhad, S. Salehnasab, Green synthesis of biscoumarin derivatives catalyzed by recyclable CuO–CeO2 nanocomposite catalyst in water, Res. Chem. Intermed., 41 (2015) 5713-5721.